

Train-On-Request: An On-Device Continual Learning Workflow for Adaptive Real-World Brain Machine Interfaces

Lan Mei[†], Cristian Cioflan[†], Thorir Mar Ingolfsson[†], Victor Kartsch[†],
Andrea Cossetini[†], Xiaying Wang^{*†}, Luca Benini^{‡‡}

[†]Dept. ITET, ETH Zürich, Zürich, Switzerland ^{‡‡}DEI, University of Bologna, Bologna, Italy

Abstract—Brain-machine interfaces (BMIs) are expanding beyond clinical settings thanks to advances in hardware and algorithms. However, they still face challenges in user-friendliness and signal variability. Classification models need periodic adaptation for real-life use, making an optimal re-training strategy essential to maximize user acceptance and maintain high performance. We propose TOR, a train-on-request workflow that enables user-specific model adaptation to novel conditions, addressing signal variability over time. Using continual learning, TOR preserves knowledge across sessions and mitigates inter-session variability. With TOR, users can refine, on demand, the model through on-device learning (ODL) to enhance accuracy adapting to changing conditions. We evaluate the proposed methodology on a motor-movement dataset recorded with a non-stigmatizing wearable BMI headband, achieving up to 92% accuracy and a re-calibration time as low as 1.6 minutes, a 46% reduction compared to a naive transfer learning workflow. We additionally demonstrate that TOR is suitable for ODL in extreme edge settings by deploying the training procedure on a RISC-V ultra-low-power SoC (GAP9), resulting in 21.6 ms of latency and 1 mJ of energy consumption per training step. To the best of our knowledge, this work is the first demonstration of an online, energy-efficient, dynamic adaptation of a BMI model to the intrinsic variability of EEG signals in real-time settings.

Index Terms—brain-machine interface, EEG, wearable EEG, wearable healthcare, transfer learning, continual learning, on-device learning

I. INTRODUCTION

Brain-Machine Interfaces (BMIs) bridge the communication gap between users and devices by utilizing brain signals such as electroencephalography (EEG). Beyond the usage in laboratories and hospitals, the recent development of consumer-grade BMI is targeting a wider range of markets [1], [2]. A common category of BMI applications employs EEG signals recorded while subjects use their motor functions, i.e., Motor Movement (MM), or imagine the movements, i.e., Motor Imagery (MI), of body parts such as hands, feet, or tongue [3], [4]. These approaches could enable a wide range of BMI applications, such as automatic gaming [5] and rehabilitative robotics [6].

Such systems commonly rely on pre-trained models [5], yet exposure to novel usage conditions (i.e., sessions) or novel subjects leads to performance degradation over time [7].

Current BMI systems lack hardware and learning mechanisms to learn from the dynamic nature of EEG signals and train the models at the edge. Nevertheless, adapting to the user-specific, on-site conditions is crucial for intelligent systems in order to preserve their accuracy [8], [9]. Specifically, real-time, on-device adaptation is necessary to mitigate inter-session variability for EEG-based BMI systems [10], [11].

Recently, Wang et al. [10] proposed a chain-Transfer Learning (TL) framework that enables online finetuning with an initial calibration phase. A model is initially pretrained on the first session acquired for the target subject. For each subsequent session, the user is requested to record a set of training data at the beginning of the session on which the model is finetuned. Afterwards, the accuracy is evaluated on the following, remaining data of the session. While such TL finetuning strategy has been shown to increase the accuracy in novel, unseen conditions [12], the model forgets the variability of the data seen previously, i.e., the accuracy on previously learned conditions decreases over time, a phenomenon known as catastrophic forgetting [13]. Continual Learning (CL) techniques further improve long-term classification performance by mitigating catastrophic forgetting issues, yet they are still to be fully explored for EEG-based BMI applications.

An additional challenge in this context is the lengthy data acquisition process, which can cause boredom and drowsiness [14] in the subjects, as well as the tedious labeling procedure that affects user experience. Nonetheless, it is crucial to have sufficient EEG recordings, as the performance of Deep Learning (DL)-based BMI depends significantly on the amount of available data [15], [16]. Moreover, the complexity and noise of in-the-wild EEG signals cause low signal-to-noise ratio (SNR) levels [17] and further prolong the setup and data acquisition process. It is thus important to balance reasonable data acquisition time and satisfactory performance when designing BMI systems, namely, new training acquisitions should be performed only when really needed.

To address these challenges, we present a fine-grained adaptation methodology suitable for extreme-edge BMI systems. We denote our workflow as Train-on-Request (TOR), as it offers the user complete control in deciding when to initiate a learning process. The main contributions of this work are as follows:

* Corresponding author: xiayang@iis.ee.ethz.ch
We open-source release the codes: <https://github.com/pulp-bio/bmi-odcl.git>

- We propose a novel, flexible TOR workflow capable of online adaptations based on classification performance, improving the user experience through near real-time data acquisition;
- We introduce CL-based TOR to further mitigate inter-session variability. In particular, Experience Replay (ER)-based TOR achieves up to 92.33% accuracy while requiring 46.67% less training data than chain-TL workflows [10], reducing the acquisition time by 28 minutes;
- We demonstrate the suitability of TOR for edge processors, by showing improved classification accuracy in only 21.6 ms per training step and an energy consumption as low as 1 mJ on the GAP9 Microcontroller Unit (MCU).

II. MATERIALS AND METHODS

A. Dataset, Preprocessing, and Classification Model

In this work, we use the dataset introduced in [10] consisting of EEG data collected from a healthy subject over seven sessions using a wearable BMI headband based on BioWolf [18] at a sampling rate of 500 Hz. Following instructions shown on a screen, the subject performs MM tasks of left- and right-hand finger-tapping [19]. The instruction is shown for 4s on the screen, followed by a resting period of five to six seconds. We use all seven sessions of EEG data and take from each the first ten runs, each with five trials of left-hand movement and five of right-hand movement, to ensure experimental consistency, resulting in 100 trials per session for two-class (i.e., left- and right-hand MM) classification.

We preprocess the raw EEG data with a 4th order band-pass filter of 0.5–100 Hz, a notch filter to suppress 50 Hz power line interference, and a moving average filter with a sliding window of 0.25 s. We use MI-BMNet [20], the State of the Art (SoA) lightweight Convolutional Neural Network (CNN) for BMIs on ultra-low-power edge devices, shown in Table I.

TABLE I: MI-BMNet [20] architecture with depthwise (DW), pointwise (PW), and depthwise separable (DS) convolutions.

Blocks	Layers	# Filters	Size
Spatial Conv.	DW Conv. + BN	$N_k = 32$	8×1
Temporal Conv.	DW Conv. + BN + ReLU + Pool.	$N_k = 32$	1×128
DS Conv.	DW Conv.	$N_k = 32$	1×16
Dense	PW Conv. + BN + ReLU + Pool.	$N_k = 32$	1×1
	Dense	$2 \times N_k \times (1900//64)$	-

Algorithm 1 TOR workflow in novel sessions.

```

for  $subs = 1$  to  $subss$  do
  Test on subsession  $subs$ 
  if  $Acc \geq T_{Acc}$  then
    continue
  else
     $subs \leftarrow subs + 1$ 
    for  $ep = 1$  to  $eps$  do
      for  $trl$  in  $trls$  do
        Finetune on trial  $trl$  of subsession  $subs$ 

```

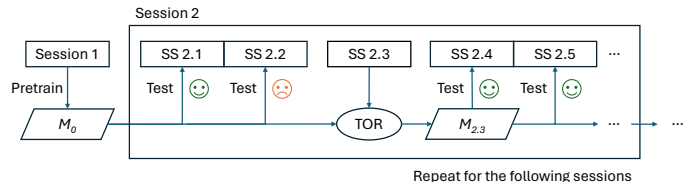


Fig. 1: The TOR workflow: we pretrain our model on Session 1. For a new session, the user utilizes the model as long as the model performance is satisfactory, exemplified here by a passing test on subsession SS2.1. When the model performance is not satisfactory, e.g., on SS2.2, the model is finetuned on the subsequent subsession SS2.3. Once the model is adapted to the new data, the user can continue to use it for the remaining session.

B. “Train-On-Request” Workflow

We propose the TOR workflow where the model is adaptively updated based on user experience. An example of the workflow is illustrated in Fig. 1. Considering different experimental sessions with varying conditions, TOR enables fine-grained evaluation within each session. When the accuracy is deemed unsatisfactory (e.g., more than one failed command out of ten attempts in controlling a BMI), the user activates TOR, which triggers a retraining phase where the model adapts to the novel condition.

Detailed implementation of TOR within a new session is described in Alg. 1. Similar to chain-TL [10], we pretrain our model on the first data session as a starting point of the workflow. The streaming data of each new session, which contains 100 trials in our dataset, is divided into $subss = 10$ subsessions (SS) of $trls = 10$ trials each. An accuracy threshold $T_{Acc} = 90\%$ models the user satisfaction with the network performance and dictates when additional learning is needed. Starting from SS_1 of a novel session, the existing model is evaluated for every incoming subsession. Once an unsatisfactory accuracy level is measured on SS_i , all trials of the SS_{i+1} are used to finetune the model for eps epochs. The evaluation process is then performed on SS_{i+2} , and the user can exploit the updated model until a new finetuning is requested (or the session is complete).

Similarly to the chain-TL methodology [10], the pre-trained model is obtained by training on first session data for 40 epochs with a learning rate of 10^{-3} . Then, we sequentially adapt the model for each of the next new sessions (i.e., six in this work), training our model for 15 epochs per subsession with a learning rate of 2×10^{-3} . We implement chain-TL as baseline following [10] and the TOR-TL based on TOR workflow.

C. Continual Learning Techniques

To improve the accuracy in new sessions while preserving knowledge acquired from previous ones, we explore CL-based approaches in addition to TOR-TL. We compare the performance of two alternatives:

- ER [21]: uses a replay buffer to store previous samples, thus preserving the knowledge over past tasks and

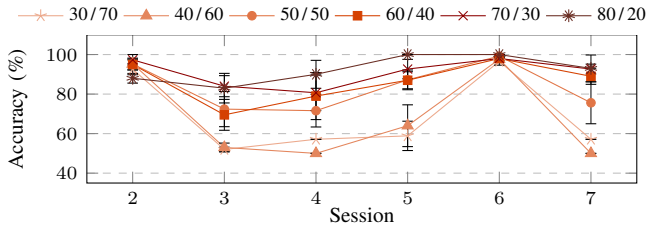


Fig. 2: Test accuracy over multiple sessions for chain-TL baseline with different train/test data splits.

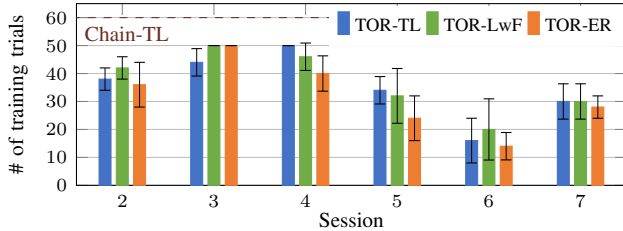


Fig. 3: Required training trials over multiple sessions for TL- and CL-based TOR workflows with $T_{Acc} = 90\%$, $trls = 10$. The horizontal dashed line represents the chain-TL baseline.

avoiding forgetting. The replay buffer is updated in each session through reservoir sampling [22]. This ensures that, in session i , the model is trained both with data from the current session, as well as with samples from all previous $i-1$ sessions. In this work, we keep ER buffer size $s_{buf} = 10$ in total throughout the workflow.

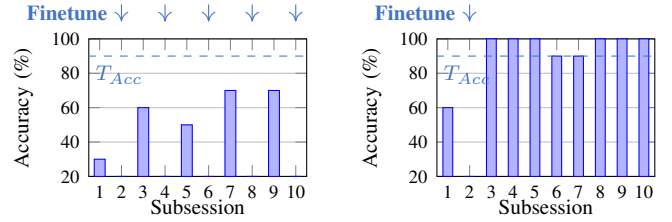
- Learning without Forgetting (LwF) [23]: uses the old model to compute the output given the new data. The output is used as regularization term in the loss function, hereby preserving previous information during finetuning process. Compared to [23], we set the distillation hyperparameter $\lambda_o = 1$ and temperature $T = 2$.

We thus implement three adaptation strategies using TOR workflow: TOR-TL, TOR-ER, and TOR-LwF. The chain-TL approach [10] is also tested to provide a baseline.

III. RESULTS

A. Chain-TL Baseline

To establish a baseline, we first explore the optimal train-test split of the acquired dataset under the chain-TL workflow [10]. Fig. 2 shows the chain-TL test accuracy over six sessions, each averaged across five runs. The measured accuracy generally increases with the number of training samples available, with the 80/20 split achieving the highest average accuracy of 92.33% across six sessions. However, this split requires 13.3 min of acquisition time for the training data for every session. To find an optimal trade-off between accuracy and training time, we note that a 60/40 split shows a satisfactory accuracy of 86.25% while reducing the acquisition time to 10 min per session. These results allow us to identify a baseline for the next TOR explorations, i.e., the chain-TL with a 60/40 split of each 100 trials acquired during a session, treating the first 60 trials as training set and the last 40 trials as test set.



(a) TOR requires adaptation every other subsession, failing to reach the desired accuracy (i.e., five subsessions, 50 training trials of 8.3 min, 56% accuracy in 16.2 s).

(b) TOR achieves the target threshold after finetuning for one subsession (i.e., one subsession, 10 training trials of 1.6 min, 93.3% accuracy in 3.2 s).

Fig. 4: Unsuccessful (a) and successful (b) TOR workflows for $subss = 10$ subsessions, $T_{Acc} = 90\%$, $trls = 10$ trials.

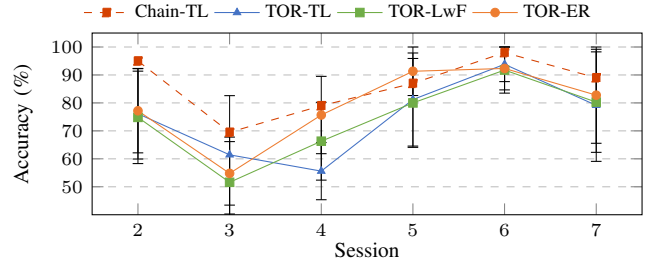


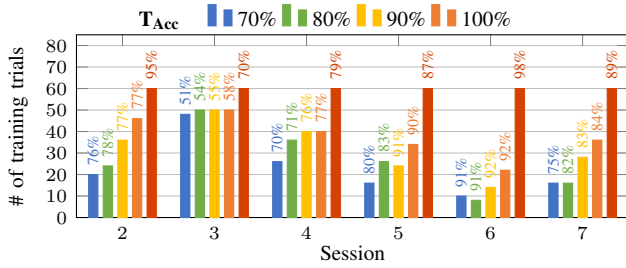
Fig. 5: Test accuracy over multiple sessions for TL- and CL-based TOR workflows, and chain-TL baseline.

B. Transfer Learning and Continual Learning through TOR

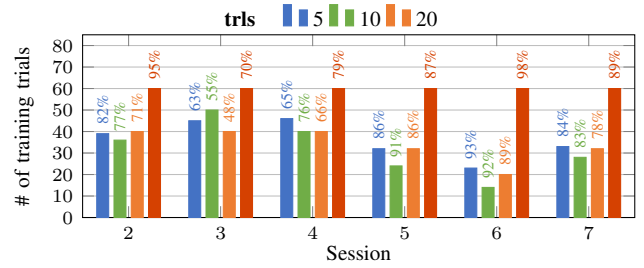
In Fig. 3, we analyze the total amount of required training trials for three learning techniques: TL-, ER-, and LwF-based TOR, compared with a chain-TL baseline. Notably, our proposed TOR strategy requires fewer training samples than chain-TL baseline. As the number of TOR training trials in each session varies, we depict the worst-case (i.e., session 3) and the best-case (i.e., session 6) scenarios in Fig. 4. Fig. 4a shows an out-of-distribution session, where the finetuned model fails to reach the desired accuracy threshold throughout the session. Conversely, Fig. 4b shows a successful scenario on in-distribution data, where TOR improves the accuracy (i.e., up to 100% within a subsession) while reducing the number of training samples (i.e., only 1.6 min of acquisition over the entire session) compared to the baseline.

When extending the intra-session analysis to an inter-session study in Fig. 3, we note that the amount of data needed to achieve satisfactory performance decreases with time, demonstrating the learning potential of our TOR workflow for long-term usage of BMI systems. Moreover, while chain-TL requires 60 training trials, the proposed ER-based TOR achieves satisfactory accuracy levels (i.e., up to 92.33% average test accuracy on session 6) using 46.67% fewer data samples. This results in a total acquisition time of 32 min, i.e., 5.3 min per session on average, for 192 trials recorded over six sessions, averaged over five runs. This is 9% (3 min) fewer than TL-based TOR and 46% (28 min) fewer than chain-TL baseline.

In Fig. 5, we further analyze the proposed TOR workflows considering the attainable classification accuracy per session. We report the test accuracy averaged over the tested subsessions within a session. When comparing the TL- and CL-based



(a) We consider $T_{Acc} \in \{70\%, 80\%, 90\%, 100\%$ for $trls = 10$.



(b) We consider $trls \in \{5, 10, 20\}$ for $T_{Acc} = 90\%$.

Fig. 6: Total number of training trials and test accuracy for TOR-ER varying the accuracy threshold T_{Acc} (a) and the number of trials in a subsession $trls$ (b). Chain-TL baseline is represented in red.

TOR approaches, ER achieves the highest average accuracy of 79% over six sessions, 4.47% over TL, while requiring the least amount of training data. We additionally note that the accuracy increases with time, reaching an average of 88.81% in the last three sessions, which is comparable with chain-TL accuracy, showing that our methodology enables the MI-BMInet backbone to gain and preserve knowledge over time. Moreover, the average Information Transfer Rate (ITR) [24] in the last three sessions is 9.0 bit/min for chain-TL and 7.6 bit/min for TOR-ER.

C. Sensitivity Analysis on TOR Constraints

Our proposed TOR workflow depends on the trial granularity within a session and on the accuracy threshold that decides the finetuning process. We measure their impact on the test accuracy and on the training trials required to achieve a satisfactory accuracy. We first fix $trls = 10$ trials in a subsession, while sweeping $T_{Acc} \in \{70\%, 80\%, 90\%, 100\%$ with ER-based TOR. When the threshold increases, so does the amount of data required, shown in Fig. 6a, as more on-site information is needed to capture the class distribution in the target domain. As depicted in Fig. 4a, imposed thresholds are not always reachable, yet with higher thresholds and more training data, we notice accuracy levels up to 58% in complex sessions and 92% in in-distribution settings.

We also analyse the number of required training trials and the achieved test accuracy under ER-based TOR, sweeping $trls \in \{5, 10, 20\}$ while keeping $T_{Acc} = 90\%$. While a coarse-grained division of trials within a subsession enables the model to access more information over the target distribution, a fine-grained division speeds up the testing and training processes. As shown in Fig. 6b, using subsessions of 10 trials ensures an optimal accuracy-training time trade-off, with an average test accuracy of 79% and an average of 5.3 min of acquisition time. Note that these parameters can be set by the users according to their acceptance of accuracy and calibration time trade-off.

D. On-Device Learning Measurements

Tailored for extreme edge MCUs, we deploy MI-BMInet and implement our On-Device Learning (ODL) routine on the GAP9 processor. Using a RISC-V Fabric Controller (FC) core as the system controller, GAP9 can delegate computational tasks to an 8-core RISC-V compute cluster, enabling efficient

parallelization of the DL workload with a power efficiency of 0.33 mW/GOP [25]. Four shared Floating Point Units (FPUs) are present in the computational cluster. Moreover, GAP9 features a shared L1 Tightly-Coupled Data Memory (TCDM) memory of 128 kB, enabling single-cycle access from the computational cores. Additional 1.6 MB L2 RAM memory and 2 MB L3 non-volatile eMRAM are present at FC level for the deployment of Deep Neural Networks (DNNs) and storage of training trials.

We freeze and quantize our MI-BMInet backbone in `int8` and deploy it using Dory [26], whilst the precision of the retrainable classifier is maintained to `fp32`. We thus benefit from the Single Instruction Multiple Data (SIMD) instructions for the integerized backbone employed only for the forward pass, whilst the backward pass and the gradient computation can be performed without loss of accuracy in single-precision floating point. We implement our proposed ODL workflow using PULP-TrainLib [27] learning library targeting PULP MCUs. By training the last linear layer on GAP9, we require only 1.08 mJ for a runtime of 21.6 ms per training step using one data trial, i.e., an average power consumption of 50.2 mW, operating at 800 mV and 370 MHz. Compared to the acquisition time of 1.6 min per subsession, TOR on-board training for 15 epochs takes only 3.2 s per subsession, enabling on-site adaptation without sacrificing user experience.

IV. CONCLUSION

This work proposes a novel TOR ODL workflow aimed for EEG-based BMI systems, which addresses inter-session variability in users through near real-time data acquisition and online finetuning to out-of-distribution sessions while also significantly reducing the training time. Addressing catastrophic forgetting, we enable adaptation to novel conditions by integrating ER-based learning in our proposed TOR workflow. We thus achieve a 46% calibration time reduction down to 1.6 min compared to the baseline, while reaching accuracy levels up to 92%. Furthermore, we deployed our ODL strategy on GAP9 MCU, showing a power consumption of 50 mW and demonstrating a modest learning cost of 1 mJ per training step within a short runtime of 21.6 ms. By providing a robust, user-friendly, and energy-efficient implementation, these results bring us closer to achieving full user acceptance of BMIs, even in challenging non-clinical scenarios.

ACKNOWLEDGMENT

This project was supported by the Swiss National Science Foundation under grant agreement 193813 (Project PEDESITE) and grant agreement 207913 (Project Tiny-Trainer), by the ETH-Domain Joint Initiative program (project UrbanTwin), and by the ETH Future Computing Laboratory (EFCL).

REFERENCES

- [1] Emotiv, “EpoC+,” <https://www.emotiv.com/epoc/>, [Online; accessed 24-May-2024].
- [2] Muse, “EEG-powered meditation and sleep headband,” <https://choosemuse.com/>, [Online; accessed 24-May-2024].
- [3] G. Pfurtscheller, “Functional brain imaging based on erd/ers,” *Vision research*, vol. 41, pp. 1257–60, 02 2001.
- [4] V. Morash, O. Bai, S. Furlani, P. Lin, and M. Hallett, “Classifying eeg signals preceding right hand, left hand, tongue, and right foot movements and motor imageries,” *Clinical neurophysiology*, vol. 119, no. 11, pp. 2570–2578, 2008.
- [5] T. N. Maleté, K. Moruti, T. S. Thapelo, and R. S. Jamisola, “Eeg-based control of a 3d game using 14-channel emotiv epoc+,” in *2019 IEEE International Conference on Cybernetics and Intelligent Systems (CIS) and IEEE Conference on Robotics, Automation and Mechatronics (RAM)*, 2019, pp. 463–468.
- [6] E. López-Larraz, A. Sarasola-Sanz, N. Irastorza-Landa, N. Birbaumer, and A. Ramos-Murguialday, “Brain-machine interfaces for rehabilitation in stroke: a review,” *NeuroRehabilitation*, vol. 43, no. 1, pp. 77–97, 2018.
- [7] C. Herff, D. J. Krusienski, and P. L. Kubben, “The potential of stereotactic-eeg for brain-computer interfaces: Current progress and future directions,” *Frontiers in Neuroscience*, vol. 14, 2020.
- [8] C. Di Napoli, G. Ercolano, and S. Rossi, “Personalized home-care support for the elderly: a field experience with a social robot at home,” *User Modeling and User-Adapted Interaction*, pp. 405–440, 2023.
- [9] D. Mukherjee, J. Hong, H. Vats, S. Bae, and H. Najjaran, “Personalization of industrial human–robot communication through domain adaptation based on user feedback,” *User Modeling and User-Adapted Interaction*, pp. 1–41, 2024.
- [10] X. Wang, L. Mei, V. Kartsch, A. Cossettini, and L. Benini, “Enhancing performance, calibration time and efficiency in brain-machine interfaces through transfer learning and wearable eeg technology,” in *2023 IEEE Biomedical Circuits and Systems Conference (BioCAS)*. IEEE, 2023, pp. 1–5.
- [11] K. R. Pyun, K. Kwon, M. Yoo, K. K. Kim, D. Gong, S. Han, and S. H. Ko, “Machine-learned wearable sensors for real-time hand motion recognition: toward practical applications in reality,” *National Science Review*, vol. 11, 11 2023.
- [12] C. Cioflan, L. Cavigelli, M. Rusci, M. de Prado, and L. Benini, “On-device domain learning for keyword spotting on low-power extreme edge embedded systems,” in *2024 IEEE 6th International Conference on AI Circuits and Systems (AICAS)*, 2024, pp. 6–10.
- [13] C. V. Nguyen, A. Achille, M. Lam, T. Hassner, V. Mahadevan, and S. Soatto, “Toward understanding catastrophic forgetting in continual learning,” *arXiv preprint arXiv:1908.01091*, 2019.
- [14] C. I. Penaloza, Y. Mae, F. F. Cuellar, M. Kojima, and T. Arai, “Brain machine interface system automation considering user preferences and error perception feedback,” *IEEE Transactions on Automation Science and Engineering*, vol. 11, no. 4, pp. 1275–1281, 2014.
- [15] A. Al-Saegh, S. A. Dawwd, and J. M. Abdul-Jabbar, “Deep learning for motor imagery eeg-based classification: A review,” *Biomedical Signal Processing and Control*, vol. 63, p. 102172, 2021.
- [16] K. M. Hossain, M. A. Islam, S. Hossain, A. Nijholt, and M. A. R. Ahad, “Status of deep learning for eeg-based brain–computer interface applications,” *Frontiers in computational neuroscience*, vol. 16, p. 1006763, 2023.
- [17] J. P. Pijn, J. Van Neerven, A. Noest, and F. H. L. da Silva, “Chaos or noise in eeg signals; dependence on state and brain site,” *Electroencephalography and clinical Neurophysiology*, vol. 79, no. 5, pp. 371–381, 1991.
- [18] V. Kartsch, G. Tagliavini, M. Guermandi, S. Benatti, D. Rossi, and L. Benini, “Biowolf: A sub-10-mw 8-channel advanced brain–computer interface platform with a nine-core processor and ble connectivity,” *IEEE Transactions on Biomedical Circuits and Systems*, vol. 13, no. 5, pp. 893–906, 2019.
- [19] H. Cho, M. Ahn, M. Kwon, and S. Jun, “A step-by-step tutorial for a motor imagery–based BCI,” in *Brain–Computer Interfaces Handbook: Technological and Theoretical Advances*, F. L. Chang S. Nam, Anton Nijholt, Ed. Taylor & Francis Group, 2018, ch. 23, pp. 445–460.
- [20] X. Wang, M. Hersche, M. Magno, and L. Benini, “Mi-bminet: An efficient convolutional neural network for motor imagery brain–machine interfaces with eeg channel selection,” *IEEE Sensors Journal*, 2024.
- [21] D. Rolnick, A. Ahuja, J. Schwarz, T. Lillicrap, and G. Wayne, “Experience replay for continual learning,” *Advances in neural information processing systems*, vol. 32, 2019.
- [22] J. S. Vitter, “Random sampling with a reservoir,” *ACM Transactions on Mathematical Software (TOMS)*, vol. 11, no. 1, pp. 37–57, 1985.
- [23] Z. Li and D. Hoiem, “Learning withemotivout forgetting,” *IEEE Transactions on Pattern Analysis and Machine Intelligence*, vol. 40, no. 12, pp. 2935–2947, 2017.
- [24] S. Frey, M. A. Lucchini, V. Kartsch, T. M. Ingolfsson, A. H. Bernardi, M. Segessenmann, J. Osielec, S. Benatti, L. Benini, and A. Cossettini, “Gapses: Versatile smart glasses for comfortable and fully-dry acquisition and parallel ultra-low-power processing of eeg and eog,” 2024. [Online]. Available: <https://arxiv.org/abs/2406.07903>
- [25] GreenWaves Technologies, “Gap9 processor,” https://greenwaves-technologies.com/gap9_processor/, [Online; accessed 24-May-2024].
- [26] A. Burrello, A. Garofalo, N. Bruschi, G. Tagliavini, D. Rossi, and F. Conti, “Dory: Automatic end-to-end deployment of real-world dnns on low-cost iot mcus,” *IEEE Transactions on Computers*, pp. 1–1, 2021.
- [27] D. Nadalini, M. Rusci, G. Tagliavini, L. Ravaglia, L. Benini, and F. Conti, “Pulp-trainlib: Enabling on-device training for risc-v multi-core mcus through performance-driven autotuning,” in *Embedded Computer Systems: Architectures, Modeling, and Simulation*, A. Orailoglu, M. Reichenbach, and M. Jung, Eds. Cham: Springer International Publishing, 2022, pp. 200–216.